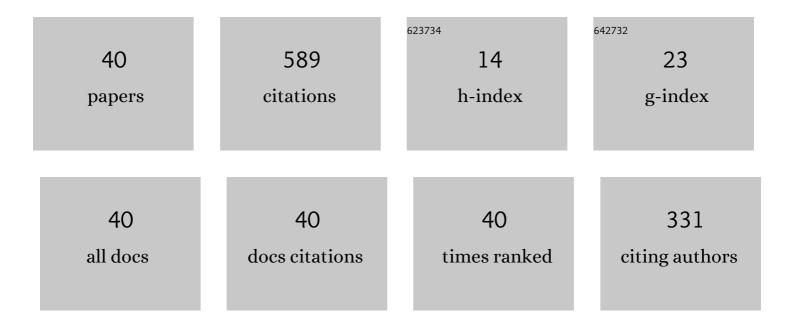
## Junjie Chen

List of Publications by Year in descending order

Source: https://exaly.com/author-pdf/6145033/publications.pdf Version: 2024-02-01



#	Article	IF	CITATIONS
1	Corrosion behaviors of four stainless steels with similar chromium content in supercritical carbon dioxide environment at 650 °C. Corrosion Science, 2019, 156, 16-31.	6.6	58
2	Characterization of interfacial reactions and oxide films on 316L stainless steel in various simulated PWR primary water environments. Journal of Nuclear Materials, 2017, 489, 137-149.	2.7	46
3	The effects of cold rolling orientation and water chemistry on stress corrosion cracking behavior of 316L stainless steel in simulated PWR water environments. Journal of Nuclear Materials, 2016, 472, 1-12.	2.7	40
4	Improving the oxidation resistance of 316L stainless steel in simulated pressurized water reactor primary water by electropolishing treatment. Journal of Nuclear Materials, 2015, 467, 194-204.	2.7	39
5	The effects of hydrogen on anodic dissolution and passivation of iron in alkaline solutions. Corrosion Science, 2015, 101, 165-181.	6.6	39
6	Oxidation behavior of Fe-20Cr-25Ni-Nb austenitic stainless steel in high-temperature environment with small amount of water vapor. Corrosion Science, 2018, 145, 90-99.	6.6	39
7	Characterization of microstructure of A508III/309L/308L weld and oxide films formed in deaerated high-temperature water. Journal of Nuclear Materials, 2018, 498, 227-240.	2.7	32
8	Characterization of microstructure, local deformation and microchemistry in Alloy 690 heat-affected zone and stress corrosion cracking in high temperature water. Journal of Nuclear Materials, 2015, 465, 471-481.	2.7	29
9	The corrosion behaviour of alloy 690 tube in simulated PWR secondary water with the effect of solid diffusing hydrogen. Journal of Nuclear Materials, 2019, 517, 179-191.	2.7	26
10	Corrosion behavior of stainless steels in simulated PWR primary water: The effect of composition and matrix phases. Corrosion Science, 2020, 177, 108991.	6.6	26
11	Properties of oxide films formed on 316L SS and model alloys with modified Ni, Cr and Si contents in high temperature water. Corrosion Science, 2016, 106, 157-171.	6.6	22
12	Comparison of oxide layers formed on the low-cycle fatigue crack surfaces of Alloy 690 and 316 SS tested in a simulated PWR environment. Nuclear Engineering and Technology, 2019, 51, 479-489.	2.3	17
13	Magnetoelectropolishing treatment for improving the oxidation resistance of 316L stainless steel in pressurized water reactor primary water. Journal of Nuclear Materials, 2019, 518, 357-369.	2.7	16
14	The effects of temperature and aeration on the corrosion of A508III low alloy steel in boric acid solutions at 25–95°C. Journal of Nuclear Materials, 2016, 480, 88-99.	2.7	14
15	Effect of zinc on the environmentally-assisted fatigue behavior of 316 stainless steels in simulated PWR primary environment. Corrosion Science, 2019, 151, 97-107.	6.6	13
16	Effect of thermal ageing on the corrosion behaviour of austenitic stainless steel welds in the simulated PWR primary water. Corrosion Science, 2020, 172, 108730.	6.6	13
17	Evaluation of thermal ageing activation energy of δ-ferrite in an austenitic stainless steel weld using nanopillar compression test. Scripta Materialia, 2020, 186, 236-241.	5.2	12
18	A magnetic field induced undulated surface and the shift of the active/passivation transition the shift of the shift of the shift of the structure of the shift o	6.6	11

Junjie Chen

#	Article	IF	CITATIONS
19	Dependence of crack growth kinetics on dendrite orientation and water chemistry for Alloy 182 weld metal in high-temperature water. Journal of Nuclear Materials, 2015, 458, 253-263.	2.7	10
20	Characterization of oxide layers formed on type 316 stainless steel exposed to the simulated PWR primary water environment with varying dissolved hydrogen and zinc concentrations. Journal of Nuclear Materials, 2021, 556, 153193.	2.7	10
21	Effects of iron content in Ni Cr Fe alloys on the oxide films formed in an oxygenated simulated PWR water environment. Journal of Nuclear Materials, 2018, 509, 29-42.	2.7	9
22	Oxidation Resistance and Stress Corrosion Cracking Susceptibility of 308L and 309L Stainless Steel Cladding Layers in Simulated Pressurized Water ReactorÂPrimary Water. Corrosion, 2021, 77, 878-895.	1.1	9
23	Supercritical-CO2 corrosion behavior of alumina- and chromia-forming heat resistant alloys with Ti. Corrosion Science, 2021, 188, 109531.	6.6	9
24	Effects of iron content in Ni-Cr- x Fe alloys and immersion time on the oxide films formed in a simulated PWR water environment. Journal of Nuclear Materials, 2017, 497, 37-53.	2.7	8
25	Corrosion behavior of Fe-based candidate accident tolerant fuel cladding alloys in spent fuel pool environment ― Effect of prior corrosion. Journal of Nuclear Materials, 2021, 548, 152845.	2.7	8
26	Effect of surface conditions and alloying elements on the early oxidation behaviour of two austenitic alloys in the pure steam environment. Applied Surface Science, 2021, 563, 150314.	6.1	7
27	Retarding effect of prior-overloading on stress corrosion cracking of cold rolled 316L SS in simulated PWR water environment. Journal of Nuclear Materials, 2017, 496, 313-324.	2.7	6
28	Effect of heat treatment on grain boundary carbides and primary water stress corrosion cracking resistance of Alloy 182 weld. Corrosion Science, 2021, 191, 109730.	6.6	4
29	On the feasibility of duplex stainless steel 2205 as an accident tolerant fuel cladding material for light water reactors. Journal of Nuclear Materials, 2021, 557, 153265.	2.7	4
30	Evaluation of thermal aging activation energies based on multi-scale mechanical property tests for an austenitic stainless steel weld beads. Materials Science & Engineering A: Structural Materials: Properties, Microstructure and Processing, 2022, 835, 142629.	5.6	4
31	Effects of surface treatments and temperature on the oxidation behavior of 308L stainless steel cladding in hydrogenated high-temperature water. Journal of Nuclear Materials, 2022, 565, 153741.	2.7	4
32	Role of residual ferrites on crevice SCC of austenitic stainless steels in PWR water with high-dissolved oxygen. Nuclear Engineering and Technology, 2020, 52, 2552-2564.	2.3	2
33	Contribution of Diffusing Hydrogen to Anodic Processes and Pitting for Iron in Chloride-Bearing Bicarbonate Solutions. Corrosion, 2022, 78, 908-926.	1.1	2
34	Distribution and Characteristics of Oxide Films Formed on Stainless Steel Cladding on Low Alloy Steel in Simulated PWR Primary Water Environments. Minerals, Metals and Materials Series, 2019, , 1965-1978.	0.4	1
35	Effects of Hydrogen on Electrochemical Behavior of a Nickel Based Alloy. ECS Transactions, 2014, 59, 455-463.	0.5	0
36	Distribution and Characteristics of Oxide Films Formed on Stainless Steel Cladding on Low Alloy Steel in Simulated PWR Primary Water Environments. Minerals, Metals and Materials Series, 2018, , 749-762.	0.4	0

JUNJIE CHEN

#	Article	IF	CITATIONS
37	Properties of Oxide Films on Ni–Cr–xFe Alloys in a Simulated PWR Water Environment. Minerals, Metals and Materials Series, 2019, , 2327-2342.	0.4	0
38	Environmentally-Assisted Fatigue Behavior of 316 Stainless Steels in Simulated PWR Primary Environment: Strain Holding, Zn-Addition, and Their Combined Effect. , 2019, , .		0
39	Properties of Oxide Films on Ni–Cr–xFe Alloys in a Simulated PWR Water Environment. Minerals, Metals and Materials Series, 2018, , 1111-1126.	0.4	0
40	Application of magnetoelectropolishing on oxidation resistance improvement of stainless steel cladding in high-temperature water. Corrosion, 0, , .	1.1	0